



# UNIVERSITÀ DEGLI STUDI DI TORINO

***This is an author version of the contribution published on:***

*Questa è la versione dell'autore dell'opera:*

[Comp Clin Pathol, 19(2): 217-220, 2010 ISSN: 16185641]

ovvero [Dezfoulian O., Sharam Jamshidi, Masoud Selk Ghaffari, M. T. Capucchio, Majid Masoudifard, Issa Jahanzad, 19. Springer, 2010, pagg 217-220]

***The definitive version is available at:***

*La versione definitiva è disponibile alla URL:*

[<http://link.springer.com/article/10.1007/s00580-009-0836-5>]

# Unusual histopathological findings in a young Pekingese dog with intrathoracic malignant peripheral nerve sheath tumour

Omid Dezfoulian & Sharam Jamshidi &  
Masoud Selk Ghaffari & Maria Teresa Capucchio  
Majid Masoudifard & Issa Jahanzad

**Abstract** This report describes intrathoracic malignant peripheral nerve sheath tumour in a Pekingese dog with unusual histopathologic findings. A 2-year-old male Pekingese dog presented with a history of pain and chronic hind limb lameness. Thoracic radiographs revealed soft-tissue opacity ventral to the thoracic vertebrae and dorsal to the aorta and base of the heart. The echo texture of the mass ultrasonographically was heterogenic, including hypo- and hyper-echoic areas within the mass, which had a well-defined echogenic wall. The owner refused further diagnostic tests, and due to a poor prognosis, the dog was euthanized. On histopathological examination, ovoid structures, known

as Verocay bodies in human schwannomas, together with the pseudo-rosette-like structures in which neoplastic cells were arranged around blood vessels, were found as the most pronounced histological feature. Immuno-histochemical examination revealed that neoplastic cells were extensively positive for both neuron-specific enolase and vimentin. To the authors' knowledge, such histopathological findings associated with malignant peripheral nerve sheath tumour in dogs have not been previously reported.

**Keywords** Malignant peripheral nerve sheath tumour . Dog

O. Dezfoulian  
Department of Pathology, Faculty of Veterinary Medicine,  
University of Lorestan, Khorramabad, Iran

S. Jamshidi : M. Masoudifard  
Department of Clinical Sciences, Faculty of Veterinary Medicine,  
University of Tehran,  
Tehran, Iran

M. Selk Ghaffari (\*)  
Department of Clinical Sciences, Faculty of Veterinary Medicine,  
Islamic Azad University-Karaj Branch,  
Karaj, Iran  
e-incili m.II;Jl;H;III .< ;Jincili orni

M. Teresa Capucchio  
Department of Animal Pathology, Faculty of Veterinary Medicine,  
University of Torino,  
Grugliasco, Torino, Italy

I. Jahanzad  
Department of Pathology, Faculty of Medicine,  
University of Medical Sciences of Tehran,  
Tehran, Iran

## Introduction

Malignant peripheral nerve sheath tumours (MPNSTs) are a rare variety of soft-tissue sarcoma of ectomesenchymal origin. MPNSTs arise from major or minor peripheral nerve branches or the sheaths of peripheral nerve fibres and are derived from Schwann cells or pluripotent cells of neural crest origin (Gupta et al. 2008). In dogs, MPNSTs have been reported in the cervical, thoracic and lumbar vertebrae and in the diaphragm and sciatic nerve (Essman et al. 2002; Okada et al. 2007; Abraham et al. 2003; Ruppert et al. 2000). In humans, it is commonly found in the lower and upper extremities, trunk, head and neck. But, intrathoracic manifestations are very rare (Park et al. 2001). MPNSTs in young dogs are uncommon; a literature search revealed no report of these tumours in young dogs except for one report of a dog with unilateral limb enlargement due to MPNST (Brower et al. 2005). The present report describes intrathoracic MPNST in a 2-year-old Pekingese dog with unusual histopathological findings.

## Case history

A 2-year-old, male Pekingese dog presented with a history of pain and chronic hind limb lameness and a week's history of progressive hind limb paresis, with faecal and urinary incontinence. The dog had no history of trauma prior to the onset of the clinical signs. The animal was bright, alert and responsive. Neurological examination revealed depressed postural reactions and pain perception in both hind limbs. The pelvic limb reflexes were present, and there was no abnormality in the thoracic, limb or cranial nerves on examination. Thoracic auscultation revealed increased respiratory sounds in the dorsal lung lobes. CBC revealed leukopenia (WBC= 3,750/(0.1) and neutropenia (2,775/(0.1). Serum biochemical profiles were within normal limits. Thoracic radiographs revealed soft-tissue opacity ventral to the thoracic vertebrae and dorsal to the aorta and the base of the heart. Tracheal bifurcation was displaced ventrally, but no abnormality was evident in the pulmonary system. The tissue mass extended from T5 to T7 of the thoracic vertebral column (Fig. 1). The echo texture of the mass was heterogenic ultrasonographically and included hypo- and hyper-echoic areas within the mass with a defined echogenic wall. The dimensions of the mass on ultrasonographic examination were 3.2x2 cm (Fig. 2). The owner refused further diagnostic tests, and due to a poor prognosis, the dog was euthanized. At necropsy, a large intradural-extramedullary mass was identified, which had grown into the vertebral canal and protruded from the right side of the T6-T7 interval space resulting in severe spinal cord compression. The mass measured 6.5x5x 3.5 cm, and had a soft, smooth well-encapsulated appearance. The tumour's cut surface was solid, brown to

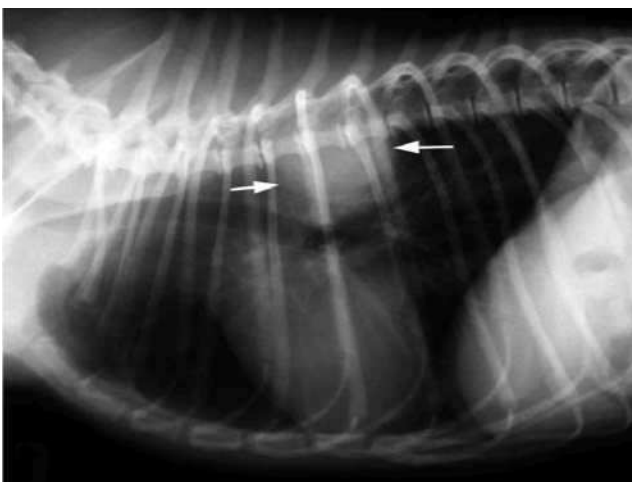


Fig. 1 Lateral radiograph of the thorax confirmed a solitary abnormal mass (arrows) of soft-tissue density which extended from T5 to T7 of the thoracic vertebral column



Fig. 2 Transverse ultrasonographic image of the dorsal thoracic region revealed a well-circumscribed heterogenic mass with a defined echogenic wall in the dorsolateral proximity of the aorta (Ao)

red in colour with conspicuous haemorrhage in most regions. Samples from the mass were processed and embedded into paraffin, sectioned at 5  $\mu$ m and stained with haematoxylin and eosin (HE).

For immuno-histochemical analysis, the following anti-bodies were applied in appropriate dilutions on sample sections: rabbit polyclonal antibodies (PoAb) against myelin basic protein MBP (Dako, Glostrup, Denmark), as well as synaptophysin SYP (Dako), and mouse monoclonal antibodies (Moab) against neuron-specific enolase NSE (Dako), vimentin (Dako), neuro-filament protein NFP (specific for 200 and 70-kDa subunits, Dako), glial fibrillary acidic protein GFAP (Dako), cytokeratin (Dako, clone MNF116), desmin (Dako), and S-100 (Dako), using the labelled streptavidin-biotin method (LSAB™ Kit, Dako). Slides were counterstained with Mayer's haematoxylin.

Two distinct regions of highly (Antoni type A) and hypocellular tissue (Antoni type B) were identified and designated as prominent histological features for this tumour (Fig. 3). The cellularly dense parts of the lesion are composed of either fusiform cells arranged in broad sheets of interlacing bundles or round and polygonal-shaped cells with a concentric arrangement around prominent blood vessels (Fig. 4). The compact groups of spindle-shaped cells were located as parallel rows at the periphery of the ovoid or Verocay body structures (Fig. 5). In the cell sparse areas, the tumour cells were embedded into the myxomatous matrix (Fig. 6). The majority of neoplastic cells, specifically those arranged around blood vessels, had abundant eosinophilic cytoplasm from well to poorly defined borders. The round to elongated nuclei were sometimes vesicular with prominent nucleoli. Mild to moderate mitotic activity was detected.

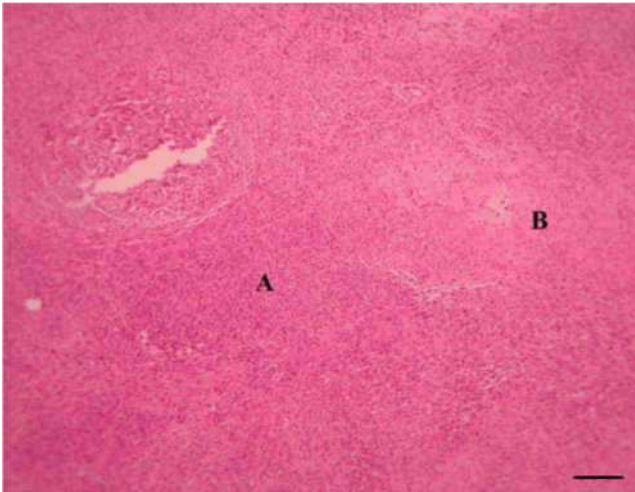


Fig. 3 Spinal cord; Antoni type A tissue of Schwann cells is highly cellular (A), consisting of elongated fusiform cells that form interwoven bundles and Antoni type B tissue with very loose vacuolated myxomatous stromal tissue (B). Haematoxylin and eosin (HE) stain. Bar=400  $\mu$ m

Furthermore, multiple foci of cartilaginous tissues as heterogeneous elements, which are often found in nerve sheath tumours, were scattered within the lesion. Massive haemorrhage was another striking microscopic feature, which occurred in many regions of the tumour mass. Extensive destruction of the parenchymal structure of the spinal cord had also occurred. The neuropil was disrupted by the presence of extremely loose pale oedema.

The vacuolated tissue moreover showed numerous dilated blood-filled vessels lined by endothelial cells with

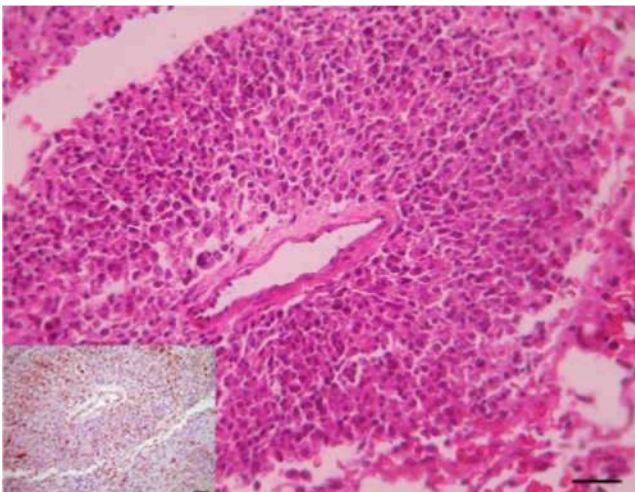


Fig. 4 Spinal cord; neoplastic cells are arranged in multiple layers oriented around the central vascular core with abundant eosinophilic cytoplasm and round to oval shape nuclei (pseudo-rosette like structure). Haematoxylin and eosin (HE) stain. Inset Neoplastic cells exhibit positive labelling for neuron specific enolase in adjacent section. SAB immuno-labelling with Mayer's haematoxylin counter stain. Bar=30  $\mu$ m

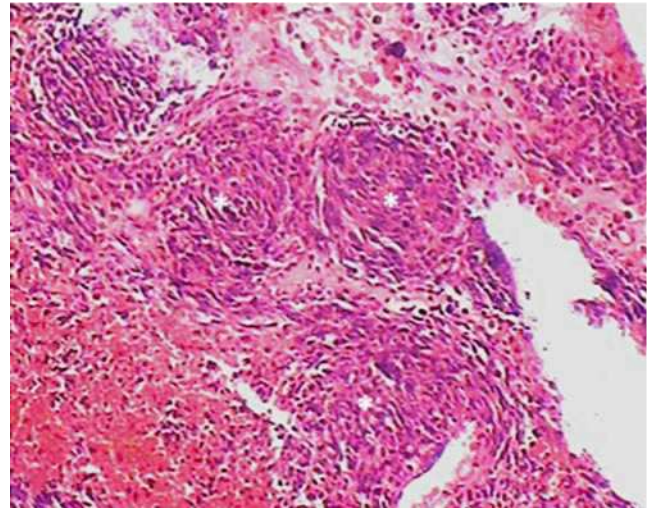


Fig. 5 Spinal cord; compact whorls of ovoid masses or Verocay bodies (asterisks), with tumour cells arranged in parallel rows and obvious haemorrhage. Haematoxylin and eosin (HE) stain. Bar=200  $\mu$ m

prominent elongated nuclei. A moderate number of extravasated red cells were detected in the parenchyma. A cellular infiltrate consisting of large numbers of macrophages with considerable amounts of vacuolated and granular cytoplasm and an ovoid or slightly pleomorphic nucleus were observed. A relatively small number of other inflammatory cells such as lymphocytes, plasma cells and rare neutrophils were also reported. The majority of neurons had degenerated and showed absence of the nucleus and Nissl substance. In the remaining neurons, which remained intact, a condensed cytoplasm

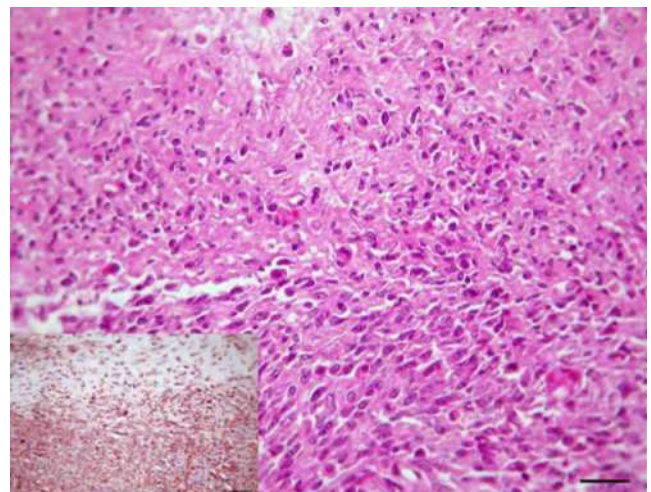


Fig. 6 Spinal cord; round neoplastic cells loosely arranged in an abundant myxoid stroma (top) in contrast to the closely packed tumour cells with a well-defined cytoplasm (bottom). Haematoxylin and eosin (HE) stain. Inset Adjacent section, where the same neoplastic cells are positive for vimentin. SAB with Mayer's Haematoxylin counter stain. Bar=30  $\mu$ m



and nucleus with marginated chromatin was observed. On immuno-histochemical staining, tumour cells showed strong positivity when labelled for NSE (Fig. 4, inset) and vimentin (Fig. 6, inset), not remarkable for S-100 and negative for NFP, MBP, SYP, GFAP, desmin and cytokeratin. The coexpression of NSE and vimentin was found in most populations of the tumour cells.

## Discussion

In this case, chronic hind limb lameness and subsequent progressive hind limb paresis were the main clinical manifestations. MPNSTs previously called schwannomas or neurofibromas are a principle cause of chronic neuro-genic lameness in dogs (Da Costa et al. 2008). Metastases of MPNST to the lungs have been reported in dogs, whilst in goats, this tumour in the thoracic vertebrae develops systemic metastases (Okada et al. 2007). In our case, however, we did not observe metastases to any organ.

In human MPNSTs, a positive labelling for S-100 is reported in 50-90% of patients, and for MBP, it is less than 50% (Kuwamura et al. 1998). Nevertheless, some reports have concluded that in all probability, the absence of S-100 positivity implies malignancy (Chijiwa et al. 2004). It was not clear in this case whether the round tumour cells, specifically those arranged around vessels, originated from precursor of schwann cells or not; however, the positive labelling for NSE and vimentin is consistent with the evidence that these cells are immature with neuronal origin, which arise from migratory neural crest stem cells (Kim et al. 2003; Chijiwa et al. 2004).

Although histological pattern of Antoni type A and B tissue are frequently reported in animal schwannomas, this is in contrast to findings from human patients. However, the presence of Verocay bodies is an important feature leading to a definitive diagnosis of this tumour (Koestner and Higgins 2002). In conclusion, to our knowledge, the

presence of these ovoid bodies has not been reported in the veterinary literature to date.

## References

- Abraham LA, Mitten RW, Beck C, Charles JA, Holloway SA (2003) Diagnosis of sciatic nerve tumor in two dogs by electromyography and magnetic resonance imaging. *Aust Vet J* 81:42^6. doi:10.1111/j.1751-0813.2003.tb11421.x
- Brower A, Salamat S, Crawford J, Manley P (2005) Unilateral limb enlargement in a dog with a malignant peripheral nerve sheath tumor. *Vet Pathol* 42:353-356. doi:10.1354/vp.42-3-353
- Chijiwa K, Uchida A, Tateyama S (2004) Immunohistochemical evaluation of canine peripheral nerve sheath tumors and other soft tissue sarcomas. *Vet Pathol* 41:307-318. doi:10.1354/vp.41-4-307
- Da Costa RC, Parent JM, Dobson H et al (2008) Ultrasound-guided fine needle aspiration in the diagnosis of peripheral nerve sheath tumors in 4 dogs. *Can Vet J* 49:77-81
- Essman SC, Hoover JP, Bahr RJ, Ritchey JW, Watson C (2002) An intrathoracic malignant peripheral nerve sheath tumor in a dog. *Vet Radiol Ultrasound* 43:255-259. doi:10.1111/j.1740-8261.2002.tb00999.x
- Gupta G, Mammis A, Maniker A (2008) Malignant peripheral nerve sheath tumors. *Neurosurg Clin N Am* 19:533-543. doi:10.1016/j.nec.2008.07.004
- Kim DY, Cho DY, Kim DY et al (2003) Malignant peripheral nerve sheath tumor with divergent mesenchymal differentiations in a dog. *J Vet Diagn Invest* 15:174-178
- Koestner A, Higgins RJ (2002) Tumors of the nervous system. In: Meuten DJ (ed) *Tumors in domestic animals*, 4th edn. Iowa State Press, Ames, pp 697-738
- Kuwamura M, Yamate J, Kotani T et al (1998) Canine peripheral nerve sheath tumor with eosinophilic cytoplasmic globules. *Vet Pathol* 35:223-226
- Okada M, Kitagawa M, Shibuya H et al (2007) Malignant peripheral nerve sheath tumor arising from the spinal canal in a cat. *J Vet Med Sci* 69:683-686. doi:10.1292/jvms.69.683
- Park JH, Choi KH, Lee HB et al (2001) Intrathoracic malignant peripheral nerve sheath tumor in von Recklinghausen's disease. *Korean J Intern Med* 16:201-204
- Ruppert C, Hartmann K, Fischer A et al (2000) Cervical neoplasia originating from the vagus nerve in a dog. *J Small Anim Pract* 41:119-122. doi:10.1111/j.1748-5827.2000.tb03178.x